Structure of the cobalt-filled missing-row reconstruction of Pt(110)

C. Klein,[1] R. Koller,[1] E. Lundgren,[2] F. Máca,[3,4] J. Redinger,[1,4] M. Schmid,[1,*] and P. Varga[1]
[1]*Institut für Allgemeine Physik, Vienna University of Technology, Wiedner Hauptstr. 8-10, A-1040 Vienna, Austria*
[2]*Department of Synchrotron Radiation Research, Institute of Physics, University of Lund, Box 118, S-221 00 Lund, Sweden*
[3]*Institute of Physics ASCR, Na Slovance 2, CZ-182 21 Praha 8, Czech Republic*
[4]*Center for Computational Materials Science, Getreidemark 9/134, A-1060 Wien, Austria*
(Received 17 March 2004; revised manuscript received 28 July 2004; published 18 October 2004)

The atomic structure of 0.5 monolayer (ML) Co deposited on Pt(110) was investigated by quantitative low-energy electron diffraction and *ab initio* density functional theory calculations, showing a pronounced inward relaxation and a filling of the missing-row sites of the Pt(110) substrate by Co atoms. Up to this Co coverage no significant intermixing of Pt atoms with Co atoms was observed by scanning tunneling microscopy, resulting in an alternating arrangement of pure Co and Pt rows.

DOI: 10.1103/PhysRevB.70.153403 PACS number(s): 68.47.De, 61.14.Hg, 68.37.Ef, 68.43.Bc

Due to the fact that ultrathin Co/Pt multilayers (Co layers thinner than 10 Å) show perpendicular magnetic anisotropy and large magneto-optical signals, they are regarded as candidates for high-density magneto-optical recording media[1] and were consequently thoroughly investigated during the last decade.[2] The origin of the perpendicular anisotropy is thought to be caused by a combination of structural and morphological effects but still not completely understood. So far the main focus of research lay on the Co/Pt(111) interface which is reported to show the largest anisotropy.[3–8] In this paper, however, we present results on the structural details of 0.5 monolayer [ML; 1 ML equals the number of Pt atoms in an unreconstructed Pt(110) plane] of cobalt deposited on a Pt(110) surface. The structural anisotropy inherent to the Pt(110) substrate renders this system particularly suitable for studying the relationship between geometry and magnetism. Moreover, since there is almost no intermixing of Co with Pt atoms at this coverage (as shown below), only missing-row sites are occupied by cobalt, resulting in alternating Co-Pt-Co rows, which build up a template that could be used for the growth of one-dimensional ordered nanostructures. Additionally, an ordered bimetallic surface like the one described above would be very attractive for studies of site-specific adsorption. Although a filling of the missing-row sites by cobalt has been observed in the early growth stages before,[9] detailed information on the exact atomic structure is still missing.

In this paper we present a quantitative low-energy electron diffraction (LEED) analysis and *ab initio* density functional theory calculations of the low-coverage $p(1\times2)$-Co/Pt(110) structure described above, supported by scanning tunneling microscopy (STM), Auger-electron spectroscopy (AES), and ion-scattering spectroscopy (ISS) results. The agreement between experimental and theoretical findings is very good indeed, further confirming the correctness of the presented values.

For our experimental study, a Pt(110) crystal was cleaned by cycles of sputtering with 2-keV Ar^+ ions, followed by an annealing step at 850 °C. According to AES measurements the sample was free from disturbing contaminations. The cobalt-filled missing-row structure was prepared by evaporating 0.5 ML of Co from a water-cooled electron beam evaporator, while the sample was kept at room temperature. The amount of deposited Co was determined using a quarz crystal microbalance and subsequently checked by ISS.

All measurements were done in Vienna in two separate UHV chambers with base pressures better than 5×10^{-11} mbar. The STM images were taken at room temperature by a customized Omicron micro-STM with an electrochemically etched W tip in constant current mode with the sample at negative voltage. Prior to all STM measurements, however, an additional chamber with a base pressure below 10^{-10} mbar was used for sample preparation. The LEED measurements were performed in the other UHV system at normal incidence of the primary electron beam using a two-grid system and video data acquisition. The LEED patterns were stored as 8-bit images and subsequently analyzed by an image processing program which extracted the *I-V* spectra for each visible beam. In order to improve the quality of the recorded images, an image processing sequence similar to the one used for astronomical charge-coupled device images[10] was implemented prior to the evaluation of the spot intensities (see Ref. 11). For the LEED calculations the TENSERLEED program package[12] was used, where an energy dependent real part of the inner potential[13] that accounts for the variation of the exchange potential with energy was implemented. This energy dependence of the inner potential and the phase shifts of the different atomic sites were calculated for the given structure. To determine the agreement between measured and calculated *I-V* curves the Pendry *R* factor[14] was chosen. The error bars given in this paper were derived from Pendry's variance,[14] namely by varying a certain parameter away from the best-fit structure until the difference between the according *R* factor got larger than this variance. To reduce the computational effort, all other parameters were fixed to their best-fit value, i.e., no subsequent reoptimization was performed. This neglect of parameter correlations is a standard procedure in today's LEED analyses and can result in a slight underestimation of the error limits.[15]

First principles density functional theory (DFT) calculations were performed using both the all-electron full-potential linearized augmented plane wave[16] code FLAIR (Ref. 17) and the Vienna ab initio simulation package (VASP).[18,19] The surface was modeled using a nine-layer single slab with vacuum on both sides for FLAIR and 9- or

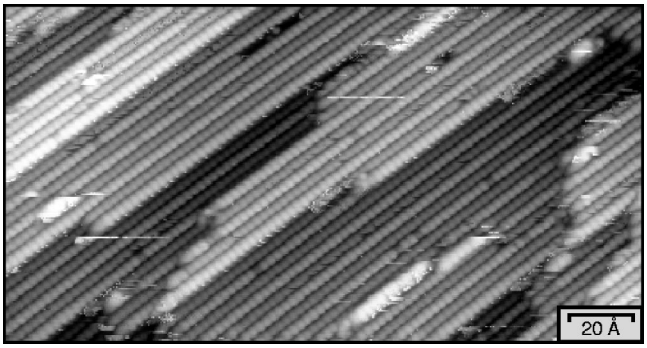

FIG. 1. STM image taken after the deposition of 0.5 ML Co on the $p(1\times2)$-reconstructed Pt(110) surface (200×105 Å^2, -0.5 mV, 4.24 nA). The image has been contrast enhanced in order to facilitate the distinction between cobalt and platinum atoms.

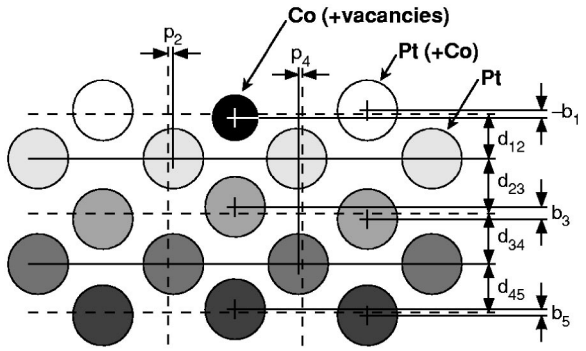

FIG. 2. Side view of the structural model considered by LEED (not to scale).

11-layer repeated slabs with ≈16 Å vacuum in between for VASP. All slabs were symmetric with respect to the middle layer, allowing us to relax four (five) layers. Two DFT potential approximations have been used: the local density approximation (LDA) according to Vosko, Wilk, and Nusair[20] and the generalized gradient approximation (GGA) according to Perdew and Wang.[21] Since the local density approximation (LDA) reproduces the experimental lattice constant of platinum with very small error [−0.3 to −0.5% (Refs. 22 and 23)] we have used the experimental value of $a=3.92$ Å (Ref. 24) for the LDA calculations. For GGA the calculated bulk value of 3.984 Å was taken. The spin-polarized calculations employed a plane-wave cutoff energy $E_{cut}=14.44$ Ry for FLAIR and 19.7 Ry for VASP. The k mesh consisted of 15 (25, including the points at the boundaries) special points in the irreducible wedge of the two-dimensional Brillouin zone for the VASP (FLAIR) calculations. The geometry was optimized until all forces were smaller than 0.01 eV/Å.

Figure 1 shows an STM image of the Co-filled Pt(110)

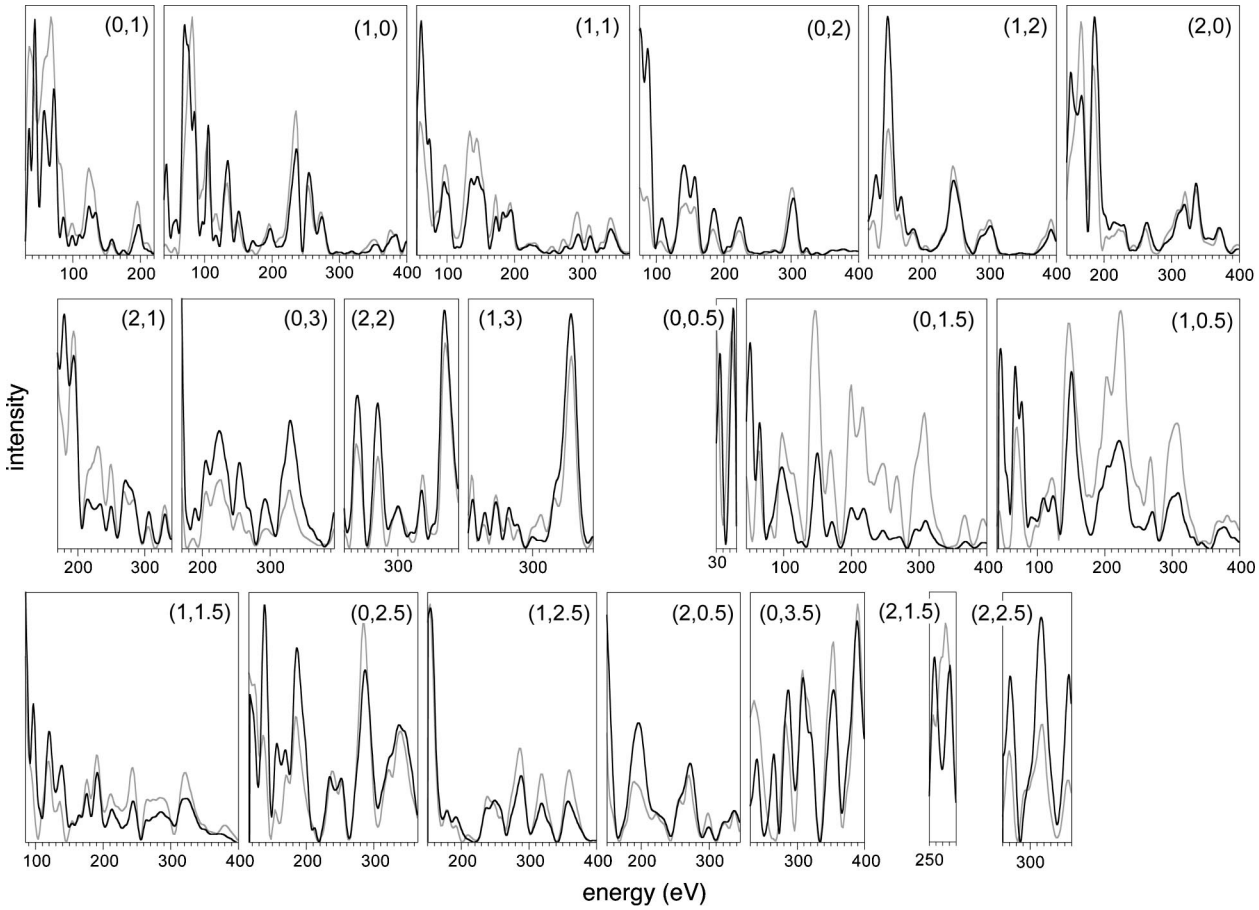

FIG. 3. Comparison between experimental (black) and calculated (gray) LEED I-V spectra of the best-fit model of the cobalt-filled missing-row structure of Pt(110). The Pendry R factor is 0.24.

TABLE I. Comparison between LEED and DFT (both LDA and GGA) results for the cobalt-filled Pt(110) structure. Here, d_{ij} denotes the averaged vertical distance between layer i and layer j and Δd_{ij} its change with respect to the bulk value. b_i and p_i represent the buckling and lateral displacements (pairing) of the atoms in layer i, respectively (buckling is positive for outwards movement of the Co row and atoms below, pairing is positive for movement towards the Co row). v_{Xi} stands for the vibrational amplitude of atom X in layer i. LDA^{9L} and GGA^{9L} denote results for a 9-layer slab obtained with FLAIR and VASP, respectively, LDA^{11L} denotes VASP results for a 11-layer slab.

Parameters	LEED	LDA^{9L}	LDA^{11L}	GGA^{9L}
v_{Pt1} (Å)	0.13±0.035	—	—	—
v_{Co1} (Å)	0.17±0.02	—	—	—
b_1 (Å)	−0.01±0.03	−0.11	−0.08	−0.05
Δd_{12} (Å)	−0.31±0.01	−0.40	−0.40	−0.39
v_{Pt2} (Å)	0.17±0.04	—	—	—
p_2 (Å)	0.09±0.05	0.08	0.09	0.11
Δd_{23} (Å)	0.14±0.03	0.17	0.17	0.23
v_{Pt3} (Å)	0.13±0.03	—	—	—
b_3 (Å)	0.06±0.04	0.06	0.07	0.06
Δd_{34} (Å)	−0.03±0.025	−0.05	−0.05	−0.01
v_{Pt4} (Å)	0.11	—	—	—
p_4 (Å)	0.04±0.04	0.02	0.02	0.01
Δd_{45} (Å)	0.00±0.024	0.00	0.00	0.04
b_5 (Å)	0.03±0.04	—	0.01	—
d_{bulk}	1.386	1.386	1.386	1.409
R_{Pe}	0.24	—	—	—

missing-row structure. As in Ref. 25 the brighter atomic species corresponds to Pt atoms, whereas Co atoms are depicted as slightly darker protrusions. A closer inspection of Fig. 1 reveils the fact that almost all missing-row sites are occupied by Co atoms, thus leveling the former "open" surface. Moreover, intermixing between cobalt and platinum in the first layer is found to be less than 10%. As a result, one can indeed identify an almost perfectly ordered structure consisting of alternating rows of cobalt and platinum.

In order to be sure to be able to treat the encountered structure with sufficient accuracy by LEED, the clean (1×2)-reconstructed Pt(110) surface was thoroughly analyzed at first. The results of this analysis (not presented in this paper) are in excellent agreement with the most recent LEED study.[22]

For the LEED I-V analysis of the Co/Pt(110) structure as shown in Fig. 1, LEED patterns starting from 30 eV up to 400 eV were recorded, with an energy step width of 1 eV. This enabled the extraction of 20 symmetry-inequivalent beam sets (ten integer and ten fractional order beams) and resulted in a cumulative energy range of 4594 eV. The only structural model considered for the LEED calculations was the one evident from the STM results, i.e., a regular Pt(110) structure, where the missing-row sites are filled with cobalt atoms. In order to account for a possible intermixing of Co with Pt atoms in the platinum rows and the existence of vacancies in the Co rows (as visible in Fig. 1), the average t-matrix approximation[26,27] was used, allowing us to treat the average atomic-site occupation and the average height of each atomic species as free parameters. Thereby, upwards or downwards movement of the few Co atoms in the top Pt row is included in the calculations. Additionally, the first five interlayer distances as well as the vibrational amplitudes of the first three layers were varied within the LEED framework. Due to symmetry reasons only buckling of the first, third, and fifth layer and pairing of the second and forth layer occurs (see Fig. 2). The imaginary part V_i of the inner potential and the vibrational amplitudes of the bulk v_{bulk}, however, were optimized full dynamically, resulting in V_i=5.5 eV and v_{bulk}=0.11 Å, respectively.

In the final structural search 18 parameters were independently varied, resulting in a Pendry R factor of 0.24 (Fig. 3). The Co occupation of the missing-row sites was determined as 90% (±15%), leaving 10% of the atomic sites vacant. Additionally a slight intermixing between platinum and cobalt atoms was observed for the otherwise pure Pt rows, which resulted in the substitution of 5% (±20%) of these Pt atoms by Co atoms with the average Co location being 0.04 Å below the Pt. The percentage of this substitution is too small, however, to have a significant impact on the first interlayer distance d_{12} or the interrow buckling b_1. Consequently, the LEED and DFT results are easily comparable. LEED and LDA show very good agreement of the atomic positions (cf. Table I) except for the vertical position of the cobalt rows, which is the main reason for different results for the first interlayer spacing. Nevertheless, both methods show a pronounced inwards relaxation of the first atomic layer of 22%(LEED)/29%(LDA), rather large lateral displacements of the platinum atoms of the second layer and considerably strong buckling of the odd Pt layers. Compared to the missing-row reconstruction of pure Pt(110),[22] the inwards relaxation of the top Pt(110) atoms and the pairing amplitude p_2 are significantly larger. We believe that the explanation is as follows: Without the presence of the Co atoms in the

troughs, the tendency of the second-layer Pt atoms towards inwards relaxation perpendicular to the {111} facets counteracts their movement into the trough necessary to make space for the first-layer Pt atom. With the small Co atoms in place, the second-layer Pt atoms will move towards the Co atoms to reduce the Co-Pt bonding distance, thereby also enabling the first-layer Pt atom to sink deeper into the surface. LDA force calculations indeed show that the pairing of the platinum atoms of the second and fourth layer is directly related to the buckling of the surface Co-Pt layer. Therefore one might also expect that the very small buckling of the first-layer atoms observed by LEED (in contrast to the LDA calculations) will be accompanied by a small buckling and pairing in the subsurface layers, but this is not the case. We rather find very good agreement of the LDA and LEED structural data in the subsurface region. This means that the reason for the very small inwards relaxation of the considerably smaller cobalt atoms found by LEED is different. We attribute at least part of the problem to the overbinding of 3*d* metals inherent to LDA, causing the cobalt atoms to move towards the second atomic layer and therefore increasing the buckling, whereas LDA is known to be almost perfect for clean platinum.[22,23] Indeed, our GGA calculations reveal a reduced buckling in the first layer but a first-layer relaxation similar to LDA, which causes a slightly different relaxation pattern in the deeper layers, thereby worsening the agreement of d_{23} with LEED. Since the system is on the verge of becoming nonmagnetic in LDA, we have also performed non-spin-polarized calculations (not shown in Table I), yielding a larger first-layer buckling due to the smaller size of a nonmagnetic Co atom, without improving the agreement of the interlayer distances with LEED. Thus, it seems hard to reconcile LEED and DFT both in the first and in deeper layers at the same level of agreement.

Although the intermixing in the surface rows (Pt-Co and Co vacancies) was found to be rather low, we cannot exclude that this intermixing, not considered in our DFT calculations, might be responsible for a small part of the LEED vs DFT discrepancies. Occasional presence of larger platinum atoms in the cobalt rows (and vice versa) changes the local geometry of the topmost layer. In the LEED analysis this effect is treated in an averaging manner, which will also tend to reduce the buckling amplitude found by LEED. Furthermore, there might be also some influence of the high step density on the quantitative LEED result. Nevertheless, we conclude that the overall agreement between both results is rather good and the R_{Pe} factor of 0.24 is satisfactory for a quantitative LEED analysis of a former "open" surface.

This work was sponsored by the Austrian *Fonds zur Förderung der wissenschaftlichen Forschung* (START program Y75), by the Grant Agency of the ASCR (Grant No. A1010214) and by RTN Project No. HPRN-CT-2000-00143 of the EC. Financial support by the Swedish Research Council is gratefully acknowledged by E.L. Special thanks go to Andreas Schmid from the *Lehrstuhl für Festkörperphysik Erlangen*, who has calculated the geometry-optimized phase shifts and energy dependence of the inner potential used in the presented LEED study.

*Electronic address: schmid@iap.tuwien.ac.at

[1] P. F. Carcia, A. D. Meinhaldt, and A. Suna, Appl. Phys. Lett. **47**, 178 (1985).
[2] D. Weller, Y. Wu, J. Stöhr, M. G. Samant, B. D. Hermsmeier, and C. Chappert, Phys. Rev. B **49**, 12 888 (1994); Y. Sonobe, D. Weller, Y. Ikeda, K. Takano, M. E. Schabes, G. Zeltzer, H. Do, B. K. Yen, and M. E. Best, J. Magn. Magn. Mater. **235**, 424 (2001); M. Yu, Y. Liu, A. Moser, D. Weller, and D. J. Sellmyer, Appl. Phys. Lett. **75**, 3992 (1999).
[3] P. Grütter and U. T. Dürig, Phys. Rev. B **49**, 2021 (1994).
[4] S. Ferrer, J. Alvarez, E. Lundgren, X. Torrelles, P. Fajardo, and F. Boscherini, Phys. Rev. B **56**, 9848 (1997).
[5] J. S. Tsay and C. S. Shern, Surf. Sci. **396**, 313 (1998).
[6] E. Lundgren, B. Stanka, W. Koprolin, M. Schmid, and P. Varga, Surf. Sci. **423**, 357 (1999).
[7] E. Lundgren, B. Stanka, M. Schmid, and P. Varga, Phys. Rev. B **62**, 2843 (2000).
[8] M. Schmid, E. Lundgren, G. Leonardelli, A. Hammerschmid, B. Stanka, and P. Varga, Appl. Phys. A: Mater. Sci. Process. **72**, 405 (2001).
[9] E. Lundgren, J. Alvarez, X. Torrelles, K. F. Peters, H. Isern, and S. Ferrer, Phys. Rev. B **59**, 2431 (1999).
[10] C. Buil, *CCD Astronomy* (Willmann Bell, Richmond, VA, 1991).
[11] R. Koller, W. Bergermayer, G. Kresse, C. Konvicka, M. Schmid, J. Redinger, R. Podloucky, and P. Varga, Surf. Sci. **512**, 16 (2002).
[12] V. Blum and K. Heinz, Comput. Phys. Commun. **134**, 392 (2001).
[13] J. Rundgren, Phys. Rev. B **59**, 5106 (1999).
[14] J. Pendry, J. Phys. C **13**, 937 (1980).
[15] S. Müller, Ph.D. thesis, University Erlangen-Nürnberg, 1996.
[16] E. Wimmer, H. Krakauer, and A. J. Freeman, Adv. Electron. Electron Phys. **65**, 357 (1985).
[17] URL: http://www.uwm.edu/~weinert/flair.html.
[18] G. Kresse and J. Furthmüller, Phys. Rev. B **54**, 11 169 (1996); URL:http://cms.mpi.univie.ac.at/vasp/
[19] G. Kresse and D. Joubert, Phys. Rev. B **59**, 1758 (1999).
[20] S. H. Vosko, L. Wilk, and M. Nusair, Can. J. Phys. **58**, 1200 (1980).
[21] Y. Wang and J. P. Perdew, Phys. Rev. B **44**, 13 298 (1991).
[22] V. Blum, L. Hammer, K. Heinz, C. Franchini, J. Redinger, K. Swamy, C. Deisl, and E. Bertel, Phys. Rev. B **65**, 165408 (2002).
[23] A. Khein, D. J. Singh, and C. J. Umrigar, Phys. Rev. B **51**, 4105 (1995).
[24] W. B. Pearson, *Lattice Spacings and Structure of Metals and Alloys* (Pergamon, Oxford, 1967).
[25] F. Máca, W. A. Hofer, and J. Redinger, Surf. Sci. **482-485**, 844 (2001).
[26] Y. Gauthier, Y. Joly, R. Baudoing, and J. Rundgren, Phys. Rev. B **31**, 6216 (1985).
[27] F. Jona, K. O. Legg, H. D. Shih, D. W. Jepsen, and P. M. Marcus, Phys. Rev. Lett. **40**, 1466 (1978).